Article No. jmbi.1999.2958 available online at http://www.idealibrary.com on IDEAL® J. Mol. Biol. (1999) 291, 313–327

JMB

A Complete Conformational Map for RNA

Venkatesh L. Murthy[1], Rajgopal Srinivasan[1], David E. Draper[2] and George D. Rose[1]*

[1]*Department of Biophysics & Biophysical Chemistry, Johns Hopkins University School of Medicine, 725 N. Wolfe Street Baltimore, MD 21205-2105, USA*

[2]*Department of Chemistry Johns Hopkins University, 3400 N. Charles Street, Baltimore MD 21218-2864, USA*

**Corresponding author*

A simple stereochemical framework for understanding RNA structure has remained elusive to date. We present a comprehensive conformational map for two nucleoside-5′,3′-diphosphates and for a truncated dinucleotide derived from a grid search of all potential conformers using hard sphere steric exclusion criteria to define allowed conformers. The eight-dimensional conformational space is presented as a series of two-dimensional projections. These projections reveal several well-defined allowed and disallowed regions which correlate well with data obtained from X-ray crystallography of both large and small RNA molecules. Furthermore, the two-dimensional projections show that consecutive and ribose ring-proximal torsion angles are interdependent, while more distant torsion angles are not. Remarkably, using steric criteria alone, it is possible to generate a predictive conformational map for RNA.

Keywords: RNA conformation; RNA folding; RNA stereochemistry; RNA flexibility

Introduction

The construction of a plot describing the conformational flexibility of dipeptide systems by Ramachandran & Sasisekharan (1963) revolutionized the field of protein chemistry by providing a simple framework for understanding protein structure. Ramachandran and Sasisekharan calculated their plot based on the simple notion that atoms placed close enough to cause significant overlap of their electronic clouds would repel each other. Their plot, generated using this extremely simple criterion and ignoring all attractive interactions, accurately predicted the observed distribution of dihedral angles in proteins.

In the intervening 35 years, a similar framework for RNA has remained elusive. A number of possible explanations exist: the difficulty of searching the many degrees of freedom present in nucleotides, the difficulty in analyzing and presenting data of high dimensionality, and, perhaps most significantly, the belief that such a search would be meaningless without the application of sophisticated energetic criteria. Nonetheless, a series of partly successful attempts were made to apply similar thinking to nucleic acids, starting with Sundaralingam (1969). Sundaralingam attempted to correlate the conformational maps generated using two distinct methods: by analyzing the distribution of conformations observed in X-ray crystal structures, and by constructing a coarse excluded volume map by hand. The results, however, are limited not only by the small number of structures available at the time, but also by the difficulty of manually searching an eight-dimensional space.

Following Sundaralingam, several groups have attempted to resolve the former problem by analyzing larger databases of structures (Kim *et al.*, 1973; Holbrook *et al.*, 1978; de Leeuw *et al.*, 1980; Kitamura *et al.*, 1981; Kuszewski *et al.*, 1997; Beckers & Buydens, 1998; Duarte & Pyle, 1998). The relevance of this approach is limited by the completeness of the database used. Other attempts have tried to improve the quality of the conformational maps by including various energy terms (Lakshminarayanan & Sasisekharan, 1969; Sasisekharan & Lakshminarayanan, 1969; Govil & Saran, 1971a,b; Saran & Govil, 1971; Kim *et al.*, 1973; Newton, 1973; Saran *et al.*, 1973a,b; Yathindra & Sundaralingam, 1973; Perahia *et al.*, 1974a,b; Tewari 1974; Govil, 1976; Levitt & Warshel, 1978; Srinivasan *et al.*, 1980; Poltev *et al.*, 1981; Tosi & Lipari, 1981; Thiyagarajan & Ponnuswamy, 1981; Ponnuswamy & Thiyagarajan, 1981; Pattabiraman & Langridge, 1985; Pearlman & Kim, 1985, 1986b, 1988; Gabb & Harvey, 1993; Girlado *et al.*, 1998). Computational limitations continue to prevent comprehensive searching

E-mail address of the corresponding author: rose@grserv.med.jhu.edu

0022-2836/99/320313–15 $30.00/0

using energy criteria, limiting the significance of the constructed maps to special cases or to model compounds.

One success in the pursuit of a simple framework for understanding the conformational properties of RNA was the application of the concept of pseudorotation to the five-membered ring of the ribose sugar (Altona & Sundaralingam, 1972). This simplification allows accurate description of the conformation of the ribose ring in terms of two parameters, puckering phase and amplitude, rather than the five endocyclic torsion angles. Unfortunately, other simplified frameworks for describing the conformational ensemble of nucleic acids were not forthcoming.

Here, we describe the construction of a comprehensive map of possible nucleic acid structures. By omitting both electrostatics and all attractive interactions, including base-pairing and base-stacking, we ensure that no feasible conformers are omitted. This approach also avoids biases due to difficulties in searching or errors in energetic parameters. Conformational analysis was performed on five model systems: the nucleoside-5′,3′-diphosphates of the four nucleobases commonly found in RNA (adenine, cytosine, guanine and uracil bases) and a truncated dinucleotide (*O*-(1-β-amino-5-deoxy-D-ribofuranos-3-yl)-*O*′-(1-β-amino-D-ribofuranos-5-yl) -phosphate). Detailed analyses of one purine nucleotide (GDP), one pyrimidine nucleotide (CDP) and the truncated dinucleotide are presented here. Similar studies can be easily performed on related systems with deoxyribose sugars or with modifications to the nucleobases or to other moieties.

Theory

All conformations of the four nucleoside-5′,3′-diphosphates (ADP, CDP, GDP, UDP) and of the truncated dinucleotide were exhaustively searched for steric clashes using hard sphere criteria. For the mononucleotides, all seven backbone degrees of freedom, α, β, γ, ε, ζ, *P* and *A*, as well as the side-chain torsion angle χ were varied systematically (Figure 1(a) and (b)). Successive values for α, β, γ, ε, ζ and χ were generated on a 20° grid between −180° and 160°. The puckering phase parameter (*P*) was varied on an 18° grid between 0° and 342° in order to search all envelope and symmetric twist conformers. Simultaneously, the puckering amplitude parameter (*A*) was searched on a 2° grid between 30° and 50°. Test conformers were constructed using bond length and angle data described by Parkinson *et al*. (1996). For accuracy, all hydrogen atoms except the 2′-OH hydrogen were explicitly included.

The resulting $\sim 10^{10}$ test conformers were evaluated for steric clashes using the hard sphere criteria of Hopfinger (1973) (Table 1). Prior work (Creamer & Rose, 1994) has shown that scaling these values by 90% can effectively compensate for the fixed bond length and bond angle approximation employed in this study. A more severe scaling factor of 70% was substituted for atoms separated by three bonds, as is customary (Brooks *et al*., 1983). Finally, for hydrogen bond acceptor/donor pairs, Hopfinger's values were reduced by 50%. These conservative scale factors were chosen to ensure inclusion of all possible allowed conformers.

Table 1. van der Waals radii

Atom type	Radius (Å)
H	1.05
C (sp^2)	1.50
C (sp^3)	1.65
N (sp^3)	1.35
O (sp^3)	1.50
O (sp^2)	1.35
P	1.75

Radii for the atom types employed in this study are taken directly from those described by Hopfinger (1973). For hydrogen atoms, Hopfinger uses a range of values between 1.05 and 1.25. We employ the lower limit of this range to avoid discounting any allowed conformations. Hopfinger does not provide a radius for sp^3-hybridized oxygen atoms (only for hydroxyl groups); we have adopted a radius 1.5 Å, consistent with his other values. Radii were scaled by 50% for H-bond donor/acceptor gains, 70% for atom gains separated by three bonds and 90% for all other atom gains.

A nine-dimensional search of truncated dinucleotide conformations was conducted by exploring all combinations of conformations that are allowed for mononucleotides (Figure 1(c)). Specifically, an eight-dimensional search of conformations allowed for GDP was repeated using a 30° grid for the six dihedral angles. A list of allowed conformations generated by this search was culled to produce sets of unique (*P*, *A*, ,ε, ζ) quadruplets and unique (α, β, γ, *P*, *A*) quintuplets which are imprinted with the steric constraints present within nucleoside-5′,3′-diphosphates. All pair-wise combinations of one quadruplet and one quintuplet were applied to the 5′ and 3′ moieties of the truncated dinucleotide conformations and screened using the same hard sphere steric criteria. Again, hydrogen atoms were included explicitly with the exception of those on the 2′-hydroxyl, 1′-amino and free 5′-methyl groups, which were omitted for maximal inclusiveness.

It is possible that the attractive interactions such as base-stacking can counterbalance the negative effects of minor steric clashes. To address this issue, the energy penalty associated with a minimally disallowed atomic overlap was calculated using the repulsive van der Waals potential from CHARMM (Brooks *et al*., 1983). The unfavorable energy associated with such a ''glancing contact'' ranges from approximately 0.5 kcal/mol for a pair of hydrogen atoms overlapping by 0.21 Å (the weakest type of exclusion considered) to several kcal/mol for contacts between more electron-dense atoms. Although glancing contacts, particularly those between hydrogen atoms, might be accom-

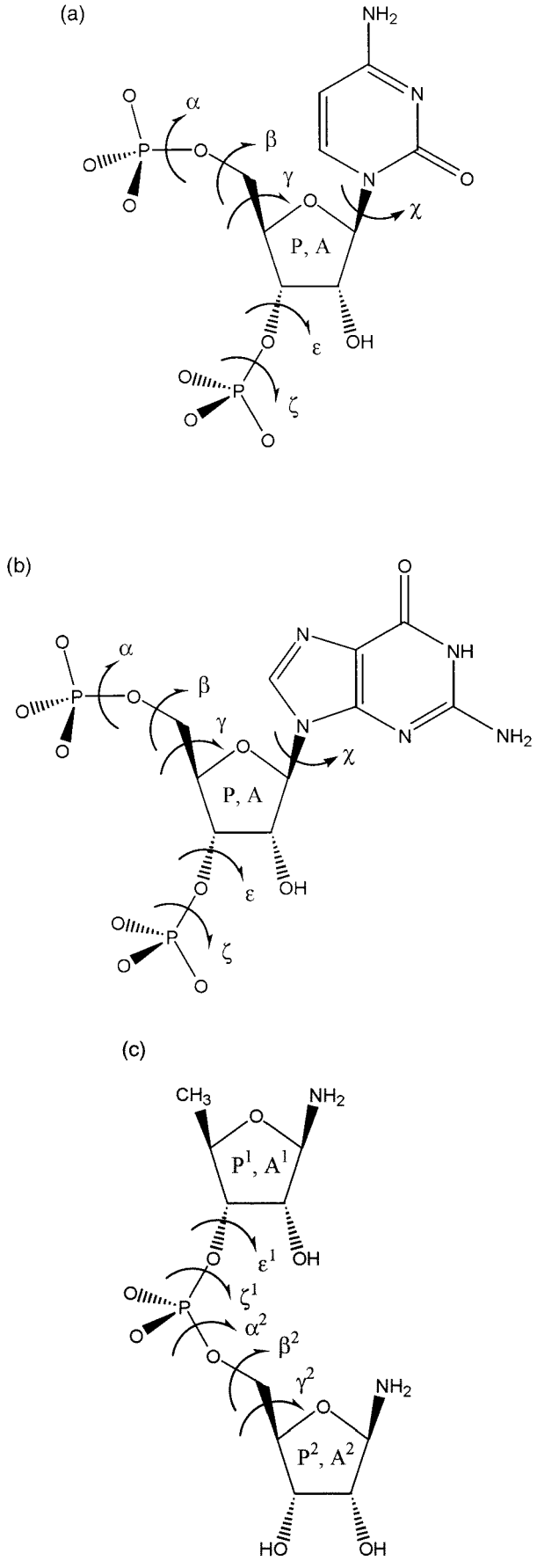

modated occasionally, closer contacts are unlikely because repulsive energies mount rapidly with decreasing inter-atomic separation.

Results

Preferred and disallowed regions (Table 2) are evident in pinwheel plots for the seven periodic parameters (i.e. α, β, γ, ε, ζ, χ and *P*) and bar charts for the puckering amplitude for both CDP and GDP (Figure 2(a) and (b), respectively). It is important to note that in this analysis the phrase ''preferred region'' refers to a conformation that is adopted with high frequency. However, these frequencies of occupation are based on sterics alone, and their corresponding regions need not be favored energetically. The allowed regions for the backbone dihedral angles (i.e. α, β, γ, ε, ζ) are strikingly similar for the two nucleotide classes, indicating that backbone and glycosidic bond conformations are largely independent.

The long P-O5′ bond allows nearly free rotation of the 5′-phosphate oxygen atoms and results in no significant preferences for the α torsion. A prominent peak (β_{II}) in the allowed region for the β-torsion angle centered about 180° places the C4′-C5′ bond in an *anti* position. Two additional highly preferred regions span the regions between *anti* and *gauche*$^+$ (β_I) and between *anti* and *gauche*$^-$ (β_{III}). The peak in the distribution of allowed values for γ that ranged from 120° to −90° is best regarded as two sub-peaks, one corresponding to eclipsed conformers (γ_I) and the other to *trans* conformers (γ_{III}). An additional allowed region for γ spans the *gauche*$^-$ configuration (γ_{II}). A single allowed region for ε spans conformations between −60 and −180°. Other conformations about the ε

Figure 1. Complete conformational searches were conducted for (a) cytidine-5′,3′-diphosphate and (b) guanosine-5′,3′-diphosphate and (c) a truncated dinucleotide (or more precisely: *O*-(1-β-amino-5-deoxy-D-ribofuranos-3-yl)-*O*′-(1-β-amino-D-ribofuranos-5-yl)-phosphate). The conformation of the two mononucleotides can be described by five backbone torsion angles (α, β, γ, ε and ζ), the ribose puckering phase (*P*) and amplitude (*A*), and the side-chain torsion angle (χ). All combinatorial conformations for these eight parameters were searched using a grid size of 20°, 18° and 2° for the dihedral angles, puckering phase and puckering amplitude, respectively. These conformations were screened for steric overlaps using the hard sphere contact radii in Table 1. A similar conformational search was conducted for the nine parameters in the truncated dinucleotide: the puckering phases (P^1, P^2) and amplitudes (A^1, A^2) of the two ribose rings and the torsion angles ε^1, ζ^1, α^2, β^2 and γ^2. Allowed conformations for GDP on a slightly coarser grid (30° for dihedrals, 18° for puckering phase, 2° for puckering amplitude) were used to generate conformations for the truncated dinucleotide. Identical steric criteria were used to screen mononucleotides and the truncated dinucleotide.

Table 2. Allowed ranges for the torsion angles and ribose pucker in a mononucleotide

	Peak I		Peak II		Peak III		Peak IV	
	Range (deg.)	Class	Range (deg.)	Class	Range (deg.)	Class	Range (deg.)	Class
α	120 to −120	Peak	−120 to −50	Peak	30 to 120	Shoulder		
β	−120 to −60	Shoulder	120 to −120	Peak	60 to 120	Shoulder		
γ	−150 to −90	Peak	30 to 60	Peak	120 to −150	Peak		
ε	170 to −50	Peak						
ζ	150 to −120	Peak	60 to 150	Peak	−120 to −30	Shoulder		
χ_{CDP}	−170 to −150	Peak	50 to 70	Peak				
χ_{GDP}	150 to −150	Peak	−120 to −60	Peak	−60 to 0	Peak	0 to 60	Peak
P_{CDP}	0 to 45	Shoulder	45 to 150	Peak	150 to 210	Shoulder		
P_{GDP}	340 to 45	Shoulder	45 to 150	Peak	150 to 240	Shoulder		

Allowed ranges as defined by examination of pinwheel and bar plot in Figure 2. These ranges, defined by clockwise rotation, correspond to statistically preferred peaks or somewhat less preferred shoulder regions.

dihedral are disallowed due to contacts between the pro-R phosphate oxygen atom and O2′ from the preceding residue. Although the allowed regions for ζ show some structure, this parameter will not be discussed in detail for CDP or GDP because its distribution is likely to be further constrained in the presence of a neighboring residue.

The allowed regions for the side-chain torsion angle χ differ markedly between CDP and GDP (Figure 2(a) and (b)). As recognized previously (Saenger, 1984), although purines are bulkier than pyrimidines, the six-membered aromatic ring in pyrimidines is more constraining than the sugar-proximal five-membered ring in purines. In pyrimidines, the carbonyl oxygen atom at position 2 is a particular source of steric hindrance. Although the nitrogen atom at position 1 in purines occupies an analogous position relative to the glycosidic linkage, it is less sterically constraining because the endocyclic bond angles are more acute in planar five-membered rings than in six-membered rings. The result is that the purine N1 atom is better separated from the ribose sugar than the pyrimidine O2 atom. Consequently, pyrimidine side-chains are constrained to a small range of *anti* conformers and a very narrow range of *syn* conformers, while purine side-chains are free to occupy intermediate conformations as well.

The range of allowed puckering phases for both CDP and GDP are similar, but not identical (Figure 2(a) and (b). Specifically, the allowed puckering phases for CDP are limited to those between 0° and 180°, while values between 340° and 0° and between 180° and 230° are tolerated, but not

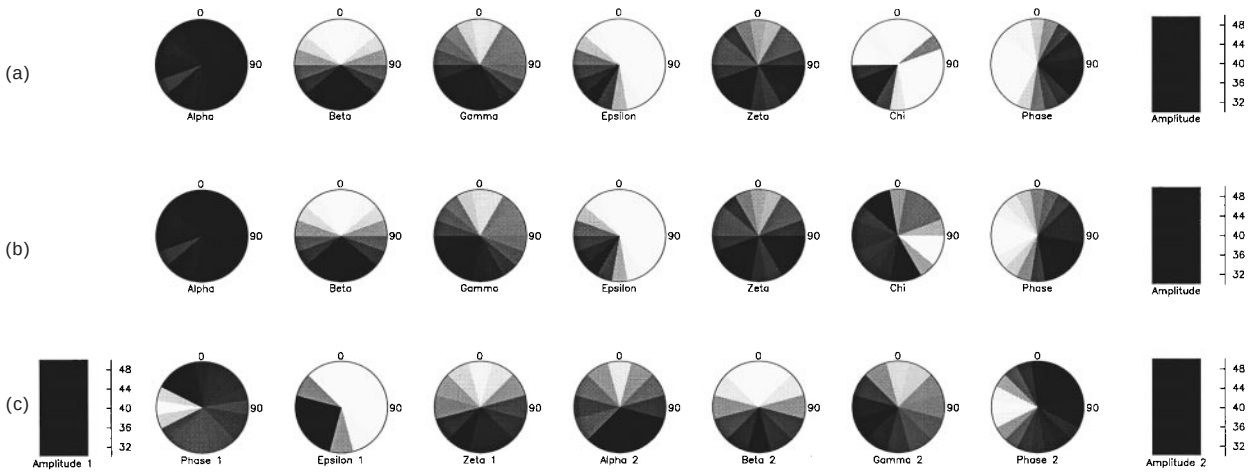

Figure 2. Preferred values of the conformational parameters for (a) CDP, (b) GDP and (c) a truncated dinucleotide in pinwheel plots for the dihedral angle and puckering phase and bar plots for puckering amplitude. The preferred regions are summarized in Table 2. The coloring is graduated from the most preferred region in black to disallowed regions in white. Although conformational preferences for backbone dihedral angles in the two mononucleotide classes are similar, the range of allowed χ values is substantially larger in purines than in pyrimidines. The permitted region for the ribose puckering phase parameter is also somewhat broader for purines. The additional conformational constraint in pyrimidines arises from the broader endocyclic angles in the six-membered aromatic ring, as has been recognized previously (Saenger, 1984). The α and ζ torsion angles describe the conformation of the 5′ and 3′-phosphate groups, respectively, and are relatively free of conformational constraints in the two mononucleotides. In the truncated dinucleotide, however, there are significant constraints on the conformation of ζ^1 and α^2. Additionally, the preferred ribose puckering phase is shifted from O4′-*endo* towards C3′-*endo*/C2′-*exo*. No significant preferences in the ribose puckering amplitude parameter are seen in any of the molecules examined.

preferred, for GDP. Essentially, avoided puckers that are those that juxtapose the 1′ and 4′ substituents: O4′-*exo*, C1′-*endo* and C4′-*endo*. Conversely, the most preferred conformation places the sugar in the O4′-*endo* configuration, maximizing separation between the 1′ and 4′ substituents. Experimental data suggest that this conformation is not favored over C3′-*endo* and C2′-*endo*. This has been attributed (Levitt & Warshel, 1978) to the observation that bond angles for out-of-plane atoms are reduced, a factor not considered in this study. There is little information on the distribution of allowed puckering amplitudes as determined by steric criteria alone (Figure 2(a) and (b)). Previous studies have shown that the electronegativity of the pentose substituents has a greater influence on the puckering phase and amplitude than the size does (Guschlbauer & Jankowski, 1980).

While one-dimensional presentations such as those in Figure 2 are informative, additional insights into the underlying stereochemical code are gained by examining higher dimensional projections of the eight dimensional conformational space spanned by mononucleoside-5′,3′-diphosphates. Two-dimensional projections were constructed by tabulating the allowed conformers in matrices for all pairs of parameters. For example, every time an allowed conformer with $\beta = 60^\circ$ and $\gamma = -180^\circ$ was encountered, the appropriate cell in the β-γ matrix was incremented. The 28 resulting matrices for each nucleotide were then contoured to reveal allowed and disallowed regions (Figure 3). Little stereochemical information is present in the matrices for the torsion angles α and ζ, because the long phosphorous-ester oxygen bonds allow relatively free rotation of the terminal phosphate. These two parameters will be discussed below in the context of the truncated dinucleotide.

Because only simple steric criteria were employed to discriminate between allowed and disallowed conformations, all allowed conformations are equivalent. The contouring of the conformational maps delineates statistical preferences for certain regions among the allowed conformers based solely on their frequencies of occurrence. Consequently, the contours do not indicate anything about the relative energies of allowed conformers.

The ten pairs of two-parameter projections catalog the complete range of conformations accessible to nucleoside-5′,3′-diphosphates (Figure 3). These distributions show good agreement with the overlaid experimental data from 97 X-ray crystal structures (549 guanosine and 481 cytidine residues, Table 3). Few data points lie outside sterically allowed regions, and most of these are from lower resolution structures (red points) and crowd to the edges of allowed areas. Conversely, nearly all of the points obtained from the highest resolution structures (blue points) lie well inside the allowed areas, typically in highly preferred regions.

Overall inspection of the plots reveals that some, but not all, of the five parameters are interdependent. For example, in the β-ε plot (Figure 3(c) and (d), the distribution of allowed β angles is largely independent of the value of ε. As such, this projection approximates a simple combination of the individual one-dimensional projections for β and ε. Conversely, the β-γ plot exhibits a strong interdependence between the β and γ torsion angles (Figure 3(a) and (b)). Essentially, several conformations about the β torsion angle, that are allowed in the one-dimensional projections (figure 2),

Table 3. Crystal structures used

NDB ID	Res (Å)	NDB ID	Res (Å)	NDB ID	Res (Å)	NDB ID	Res (Å)	NDB ID	Res (Å)
ar0001	2.30	arn035	2.25	pr0002	2.80	ptr005	2.90	urb001	0.80
ar0002	2.50	drb002	0.90	pr0003	2.86	ptr008	3.00	urb003	1.00
ar0004	2.50	drb003	1.00	pr0004	2.60	ptr009	2.60	urb008	1.00
ar0005	1.80	drb005	0.80	prv001	3.00	ptr010	2.70	urb016	0.86
ar0006	1.90	drb007	1.34	prv002	1.92	ptr011	3.00	urc002	0.95
ar0008	2.10	drb008	0.85	prv003	2.70	ptr012	2.70	urf042	1.40
arb002	0.80	drb018	1.10	prv004	2.80	ptr016	2.38	url029	2.64
arb003	1.10	drbb01	1.10	prv006	2.70	trna03	3.00	url050	2.40
arb004	0.89	drbb09	1.30	prv007	2.80	trna04	2.70	url051	2.30
arb005	0.85	drbb11	1.54	prv008	2.80	trna05	3.00	url064	1.50
arf0108	1.76	drbb12	1.14	prv009	3.00	trna06	3.00	url069	3.00
arfs26	1.30	drbb13	1.14	prv010	2.80	trna07	3.00	urt068	3.00
arh063	2.90	drbb14	0.86	prv020	1.81	trna08	3.00	urx053	2.50
arh064	1.80	drbb15	1.09	prv021	2.90	trna09	3.00	urx057	3.00
arh074	1.46	drbb16	1.30	pte003	2.25	trna10	2.50	urx058	3.00
arhb90	2.52	drbb17	1.34	ptr001	2.80	trna12	3.00	urx059	3.00
arl037	2.00	drbb19	1.34	ptr002	2.80	uhx026	2.60	urx063	2.40
arl048	1.80	drd004	1.00	ptr003	2.50	ur0002	2.10	urx067	2.90
arl062	2.60	pde0134	2.20	ptr004	2.90	ur0004	1.60	urx075	1.30
arm0107	1.80	pr0001	2.80						

All X-ray crystal structures determined to 3.0 Å or higher resolution which contain RNA in the Nucleic Acid Database (NDB) were utilized (Berman *et al.*, 1992). For simplicity, hybrid RNA-DNA chains and duplexes were excluded. The NDB ID codes and resolution for these structures are listed. Values for the conformational parameters α, β, γ, ε, ζ, χ, *P* and *A* were calculated for all RNA residues in these structures and are plotted in Figures 3 and 5.

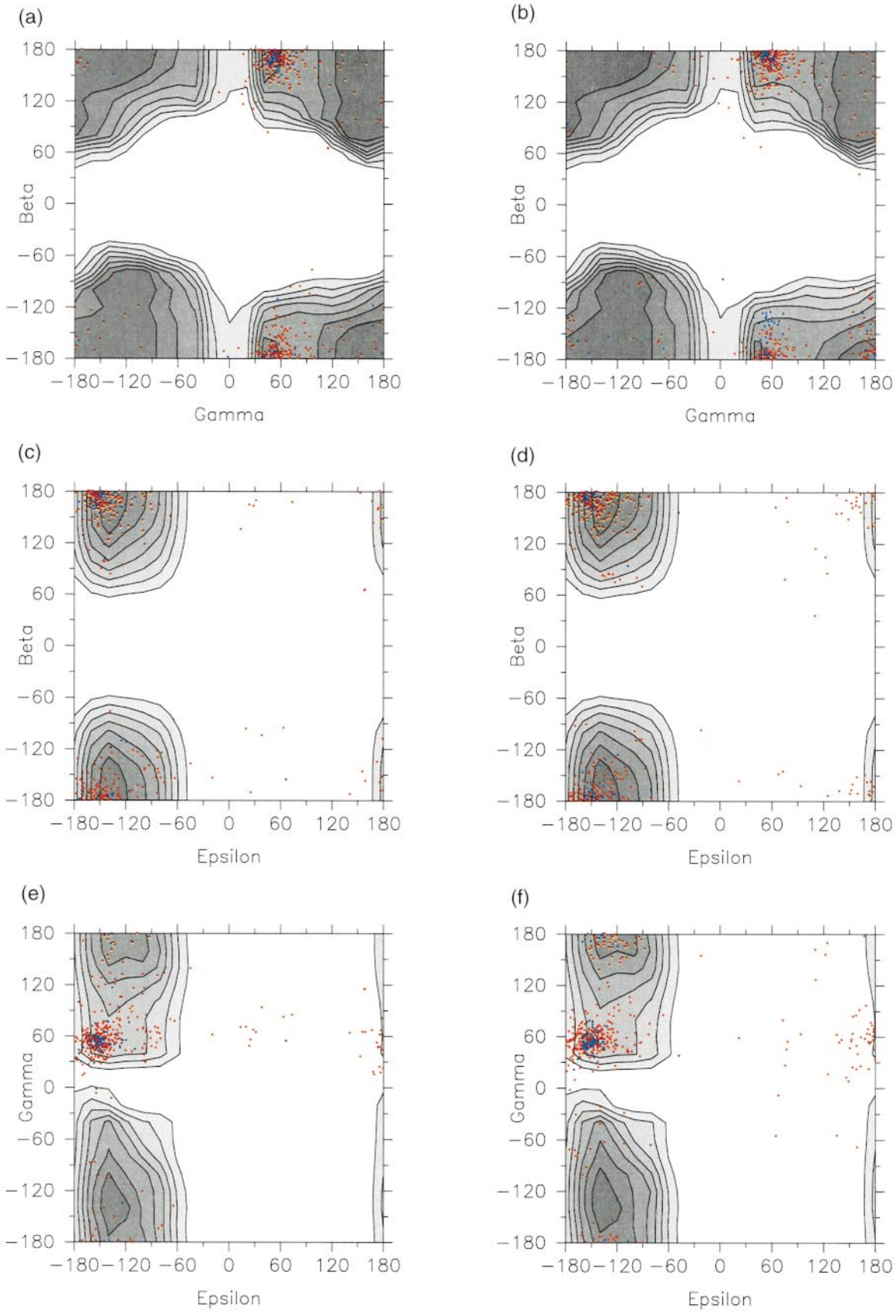

Figure 3 (*legend shown on page 321*)

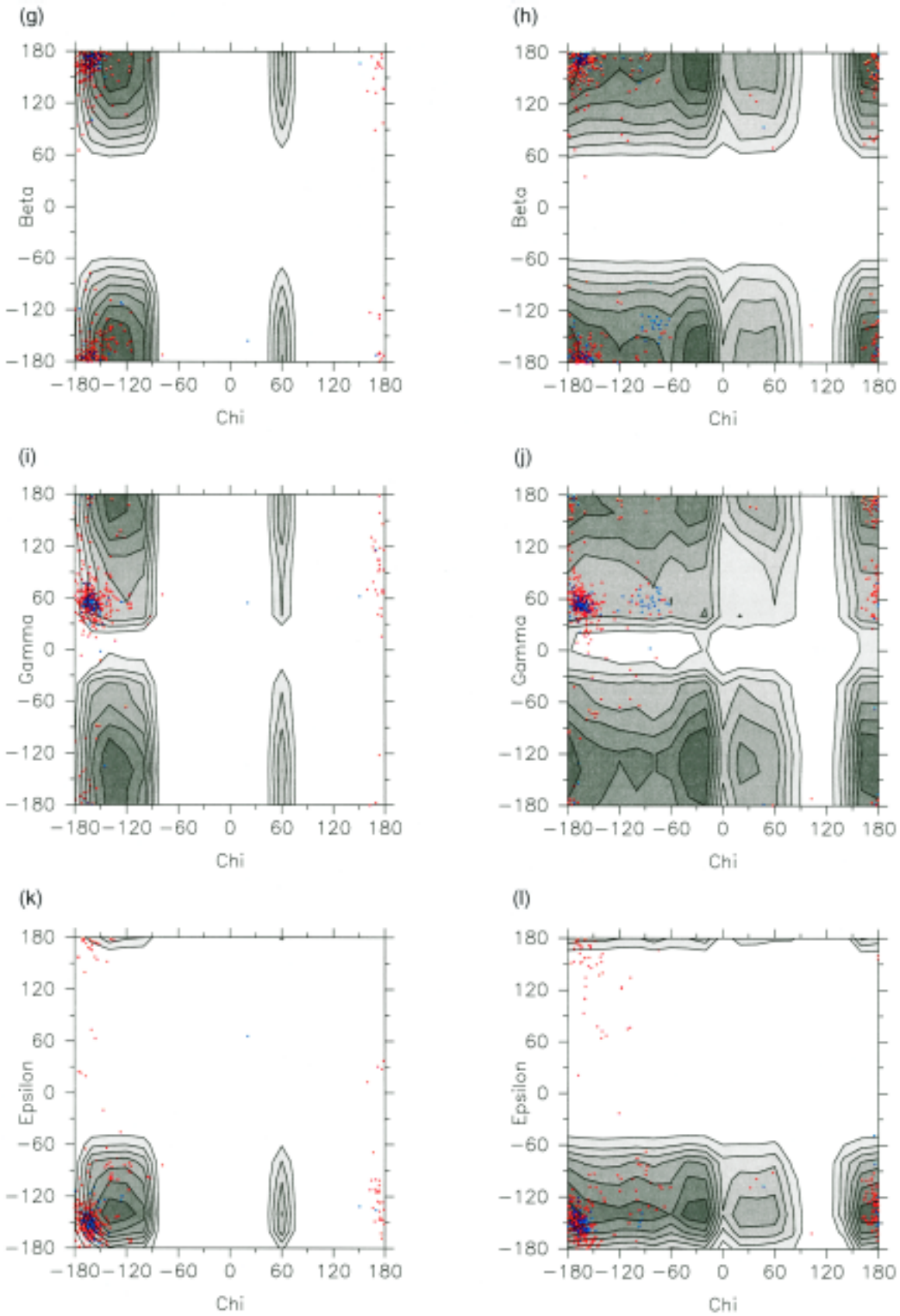

Figure 3 (*legend shown on page 321*)

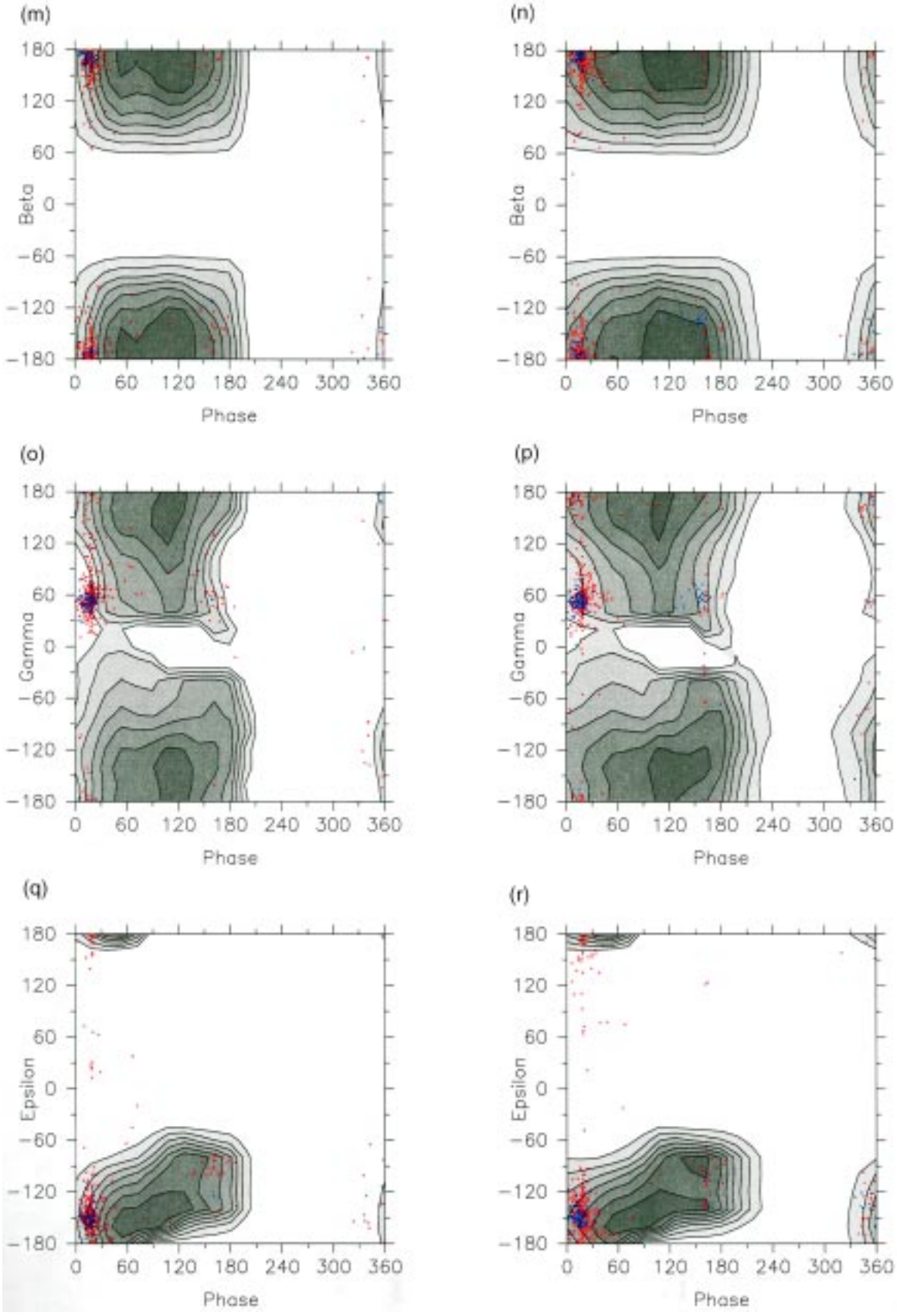

Figure 3 (*legend shown on page 321*)

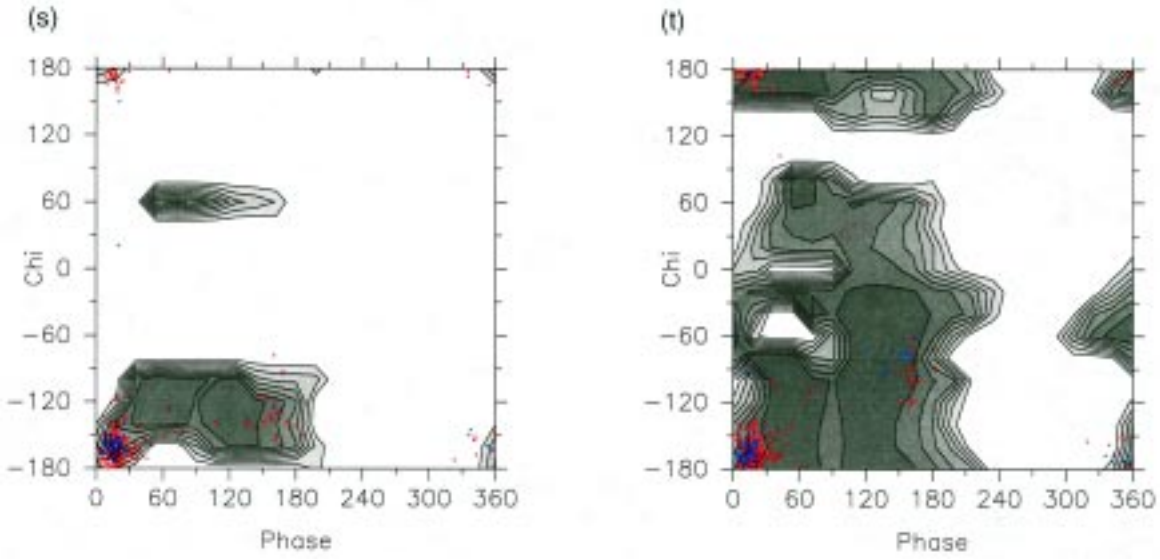

Figure 3. Well-defined, preferred conformational regions are apparent in two dimensional projections of the eight-dimensional conformational space available to cytidine-5′,3′-diphosphate (a), (c), (e), (g), (i), (k), (m), (o), (q) and (s)) and to guanosine-5′,3′-diphosphate ((b), (d), (f), (h), (j), (l), (n), (p), (r) and (t)). All pair-wise combinations of the parameters β, γ, ε, χ and *P* for each of the two nucleotide classes are plotted. As there is little information in the preferences for the conformations about the α and ζ torsion angles and the ribose puckering phase, they are omitted here. The plots contours are graduated from completely disallowed in white to most preferred in grey. We emphasize that the contours indicate statistical preferences and not energetic differences. Because of minor artifacts in contouring, grid points immediately outside the lowest contour level are usually allowed despite being colored white. Conformational parameters extracted from high resolution X-ray crystal structures (see Table 3) are overlaid for validation. Although a small fraction of points from structures with resolution between 2.5 and 3.0 Å (red) lie in regions predicted to be disallowed, almost none are found among structures at 2.5 Å or better (blue).

become disallowed for certain conformations about the γ torsion, and *vice versa*. Accordingly, the β-γ plot is not a simple composite of the allowed regions for each of its constituent angles. All interdependencies present in CDP and GDP are summarized in Figure 4. Generally, parameters which describe the conformation about non-consecutive bonds that are not both immediately proximal to the ribose ring (e.g. β-χ and β-ε), are not interdependent. Parameters which describe consecutive bonds (i.e. β and γ) or those that describe the motion of the relatively rigid ribose ring system and the bonds immediately proximal to it (i.e. γ, χ, ε and P), are interdependent. These pairs will be discussed further.

There are two well-distinguished peaks in the β-γ plots for both pyrimidines and purines (Figure 3(a) and (b)). Peak $\beta\gamma_I$ corresponds to a conformer in which the C5′-C4′ bond is in a *gauche*$^-$ conformation, placing the O5′ atom over the *endo* face of the ribose ring. Because the 5′-phosphate group is in close proximity to the ribose ring in this conformation, an *anti* conformation about the β dihedral is necessitated. This class of conformers is heavily populated in X-ray crystal structures of RNA molecules and corresponds to the canonical values for *A*-form RNA.

A broader allowed region is more sparsely populated with structural data. This region contains two classes of conformers. In the first ($\beta\gamma_{II}$), the γ torsion angle is in the *trans* configuration separating the 5′-phosphate and ribose rings. Here, positive values for the β torsion are preferred because negative values orient the 5′-phosphate towards the O4′ edge of the ribose ring. The other class of conformers ($\beta\gamma_{III}$) centers about a value of −120° for the γ torsion, causing the O5′ atom to eclipse the H4′ atom. Although eclipsed conformations are generally disfavored, they can be accommodated when one of the atoms is hydrogen. Here, negative values for β are preferred to avoid clash between the 5′-phosphate and O3′ and, to a lesser extent, the 3′-phosphate group.

The γ-ε plots (Figure 3(e) and (f)) for both purines and pyrimidines have a peak ($\gamma\varepsilon_I$) and a broad plateau region ($\gamma\varepsilon_{II}$). The plateau is comprised of the region corresponding to γ in the *gauche*$^-$ configuration and ε in configurations between *gauche*$^+$ and *trans*. The γ and ε values for *A*-form RNA fall within this region. The peak ($\gamma\varepsilon_I$) places the ε dihedral in an eclipsed configuration (−120°), where conformations from *trans* to eclipsed configuration are accessible to γ. The distortion in these plots is largely due to strong coupling between γ and *P* and between ε and *P* (see below) as the 5′ and 3′-phosphate groups can only interact at certain values for β.

The distribution of allowed γ, χ pairs (Figure 3(i) and (j)) shows that these are nearly independent. Essentially, pair-wise combinations of regions that

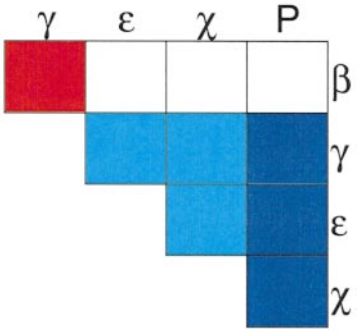

Figure 4. The two-dimensional plots in Figure 3 show that some, but not all, parameters are interdependent. Many of the plots, such as the β-ε projection (Figure 3(c) and (d)), are simple combinations of the allowed regions for the constituent individual parameters in Figure 2. Such pairs are independent (white). Parameters which describe the conformation about consecutive bonds (red) are interdependent as are those which describe the conformations ribose system and the bonds proximal to it (blue and cyan). For example, the β-γ plot (Figure 3(a) and (b)) is not merely a simple combination of the one-dimensional data for these two torsion angles (Figure 2); instead the allowed values for the β torsion angle are dependent on the conformation of the neighboring γ torsion, and *vice versa*. Torsion angles which describe rotation about bonds proximal to the ribose ring (i.e. γ, ε and χ) are all strongly dependent on the ribose puckering phase (blue) and weakly dependent on each other (cyan). The γ-ε, γ-χ and ε-χ projections (Figure 3(e), (f), (i), (j), (k) and (l)) suggest that the weak apparent interdependence of these parameters is the product of strong couplings to the relatively rigid ribose ring.

are allowed for γ and χ individually are all allowed, although the edges of these regions are slightly irregular in places. Allowed regions for ε and χ (Figure 3(k) and (l)) show essentially no interdependence for CDP, and only slight distortion of the edges of allowed regions for GDP. As for γ and ε, the distortions in both the γ, χ and ε, χ distributions arise largely from strong coupling of the three dihedrals to the puckering phase and not from direct interactions between the groups.

Allowed regions of the γ-P (Figure 3(a) and (p)) and ε-P (Figure 3(q) and (r)) plots are similar for both CDP and GDP. It is apparent, however, that the sterically preferred values for both ε and γ are sensitive to the puckering phase. Although the χ-P plots (Figure 3(s) and (t)) are different for the two nucleotides examined, both demonstrate a strong coupling between χ and the puckering phase. The canonical *A*-form values do not correspond to the most highly preferred regions on any of these plots. However, it has been previously recognized that puckering phase depends more on the electronegativity of the ribose substituents than on steric hindrance (Guschlbauer & Jankowski, 1980).

Higher order than pair-wise interdependencies are formally possible. The four parameters γ, χ, ε and P are all mutually pair-wise interdependent, raising the possibility of third or fourth-order interdependencies among members of this group. However, qualitative assessment of the magnitude of interdependence in each case indicates that some pairs (γ-P, χ-P and ε-P) are more strongly interdependent than others (γ-ε, γ-χ and ε-χ), suggesting that the weak interdependencies of γ-ε, γ-χ and ε-χ arise largely from the strong interdependence between each of those three parameters and the ribose puckering phase. This hypothesis is consistent with the observation that direct interactions between the side-chain, 3′ and 5′-phosphate groups are more limited than interactions between these groups and the ribose ring.

Analysis of the truncated dinucleotide uncovers additional constraints that are absent from nucleoside-5′,3′-diphosphates, but are present in larger RNA-like compounds. Figure 2(c) shows pinwheel and bar plots for the nine parameters present in the truncated dinucleotide: P^1, A^1, ε^1, ζ^1, α^2, β^2, γ^2, P^1 and A^2. Several of the parameters (i.e. A^1, ε^1, β^2, γ^2 and A^2) have distributions resembling those for mononucleotides. The distributions of allowed values for the two puckering phases (P^1 and P^2) are flatter than in GDP, and their peaks are shifted. Notably, the allowed regions for ζ^1 and α^2 are reduced significantly in the truncated dinucleotide relative to CDP and GDP.

Using these data, it is possible to define allowed regions for ζ^1 and α^2 (Table 2). There are three allowed regions for α^2: two peaks (α_I and α_{II}) and a shoulder (α_{III}). The peaks correspond to *trans* (α_I) and *gauche*$^+$ (α_{II}) conformations about the P-O5′ bond. The *trans* conformation is preferred over the *gauche*$^+$ conformation because it orients neighboring nucleotides in opposite directions. Canonical *A*-form RNA adopts the *gauche*$^+$ conformation, however, placing neighboring nucleotides in an orientation consistent with base-stacking. Another allowed region (α_{III}), corresponding to eclipsed (120°) conformations, is sparsely populated.

The allowed regions for ζ^1 consist of two peaks (ζ and ζ_{II}) and a shoulder (ζ_{III}). The most prominently preferred region (ζ_I) places the O3′-P bond in the *trans* configuration. Another highly preferred (ζ_{II}) region consists of eclipsed configurations centered at 120°. A less preferred region (ζ_{III}), consisting of conformations near *gauche*$^+$ configurations is highly populated and includes *A*-form structures. In our study, this region is less preferred than the *trans* configuration, which allows maximal flexibility for each of the two ribose moieties. However, the situation is surely different in solution because the *trans* configuration precludes stacking interactions between consecutive bases by increasing the separation between neighboring residues and orienting them in opposite directions.

In the two-parameter projections of allowed conformational space for the truncated dinucleotide (Figure 5), only certain parameters are interdependent, as is the case for mononucleotides. Significant interdependence is again observed between parameters that describe rotation about consecutive bonds (ε^1-ζ^1, α^2-ζ^1, α^2-β^2).

In the ε^1-ζ^1 plot (Figure 5(a)), each of the three allowed regions for ζ is consistent with nearly the entire range of allowed values for ε. The borders of allowed regions are significantly distorted in a number of places due to interactions between phosphate oxygens (including O5′) and the two atoms bound to C4′ (i.e. H4′ and C5′). Distortions where ζ is near 0° are due to unfavorable contacts between H3′ on the 5′-ribose group and O5′ on the 3′-ribose group. An unfavorable contact also occurs between H2′ and the pro-S H5′ in the next residue. Both of these can be alleviated somewhat when ε is near 180° or −60°. Values of ε near −60° are incompatible with ζ values near −60° and 120° because of unfavorable contacts between the pro-R or pro-S phosphate oxygen atom and C5′ of the previous residue, respectively. The values for ε and ζ in standard *A*-form RNA lie in a region that is only moderately preferred, probably due to an exaggerated preference for *trans* configurations about the ζ torsion.

The α^2-ζ^1 plot (Figure 5(b)) contains many highly preferred regions including three peaks ($\alpha\zeta_{I\text{-}IV}$) and several shoulders ($\alpha\zeta_{V\text{-}VII}$). One peak ($\alpha\zeta_I$), corresponding to *A*-form-like values for the α torsion angle, and ζ torsion values between *gauche*$^+$ and *trans*, has a shoulder incorporating ζ values from *trans* to nearly *gauche*$^-$ ($\alpha\zeta_V$). Fully *gauche*$^-$ conformations result in unfavorable contacts between the 3′-hydrogen atoms and C5′ of the neighboring ribose group. The *gauche*$^+$ configuration about the P-O5′ bond juxtaposes the O3′ and C5′ atoms from neighboring residues, and allows the ribose rings to be oriented to permit stacking interactions between neighboring bases. While the most preferred values for ζ in region $\alpha\zeta_V$ place the ribose moieties in positions too distant for base-stacking, a less preferred extension ($\alpha\zeta_{VI}$) to this region encompasses values near −60° for ζ which does permit base-stacking.

A second allowed ($\alpha\zeta_{II}$) region places the α torsion in a *trans* configuration preventing base-stacking interactions. Because of the relatively long length of the P-O5′ bond, eclipsed configurations for α near 120° are also highly preferred ($\alpha\zeta_{III}$ and ζ_{IV}). Almost all values for ζ, except those near 0°, are tolerated, although those near *gauche*$^+$ are less preferred. Previous work (Sudaralingam, 1969) recognized that repulsive effects between the lone-pair electrons on the O5′ and O3′ strongly disfavor the region in which both α and ζ are in the *trans* conformation.

Another moderately preferred region ($\alpha\zeta_{VII}$) places α in a *gauche*$^-$ configuration. In this configuration, which is poorly populated in crystal structures, ζ can adopt nearly any configuration except *gauche*$^+$, as that configuration results in close contacts between H2′ of the 5′ moiety and either or both of the H5′ atoms of the 3′ moiety.

A single large allowed region ($\alpha\beta_I$) that dominates the α^3-β^2 plot (Figure 5(f)) includes values between −120° and 120′. This configuration is preferred for both α and β because it results in the maximal separation of neighboring residues, nearly eliminating inter-residue contacts. Nevertheless, this configuration is not likely to be favored in solution because it prohibits stacking of consecutive bases. There are two sharp disallowed regions that occur when α is in the eclipsed (−120°) configuration and β is either 120° or −120°. When β is 120°, 1-5 interactions between the pro-S phosphate oxygen atom and pro-S H5′ are highly unfavorable. Similarly, −120° is disallowed for β because of contacts between the pro-S phosphate oxygen atom and pro-R H5′, and between neighboring ribose moieties.

Discussion

Complete conformational maps for mononucleoside-5′,3′-diphosphates were constructed using steric criteria alone. These maps reveal preferred conformations for five of the eight possible degrees of conformational freedom in these molecules. Additional constraints on α and ζ, present in RNA polymers but absent in mononucleotides, were elucidated in the truncated dinucleotide *O*-(1-β-amino-5-deoxy-D-ribofuranos-3-yl)-*O*′-(1-β-amino-D-ribofuranos-5-yl)-phosphate. All combinations of allowed conformations for GDP were applied to each of the two ribose moieties and the resulting complete truncated dinucleotide conformations were screened for steric clashes. Although interactions between each nucleobase and the neighboring residue were omitted, all other steric interactions were included. As such, the truncated dinucleotide serves as a reasonable upper limit model for the flexibility of diribonucleotides.

Because base-stacking interaction have been omitted, the set of allowed conformations for the truncated dinucleotide represents a superset of those conformations that will be highly populated in solution. Nonetheless, unstacked conformations are occasionally populated in RNA structures. Consequently, in order to construct a map inclusive of all conformations available to RNA, stacking interactions must be omitted. A map describing only those conformations permissive of stacking interactions would also be quite useful and is currently being developed.

Allowed regions in the resulting conformational maps are largely in agreement with data from X-ray crystal structures. Only a small proportion of points from higher resolution X-ray structures (3.0 Å or better) fall in sterically disallowed regions. The fraction of outliers from structures resolved to 2.5 Å or better is smaller yet. Most of these outliers are found to have actual steric overlaps, suggesting inaccuracies in model building rather than errors in our conformational maps (unpublished results). Others have also noted steric overlap errors in nucleic acid structures (Word *et al.*, 1999).

A number of interesting questions related to the conformational properties of nucleic acids can be

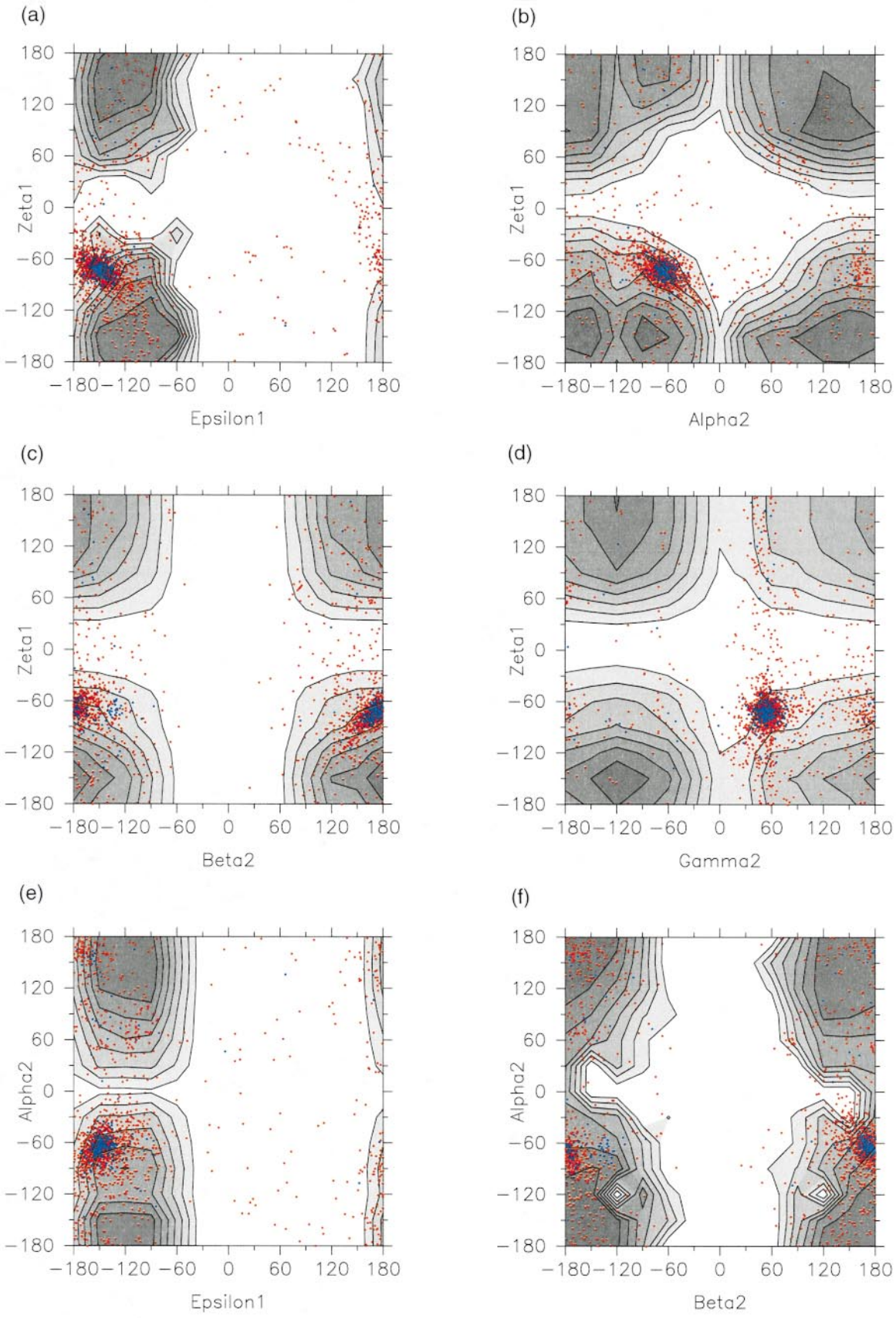

Figure 5 (*legend shown opposite*)

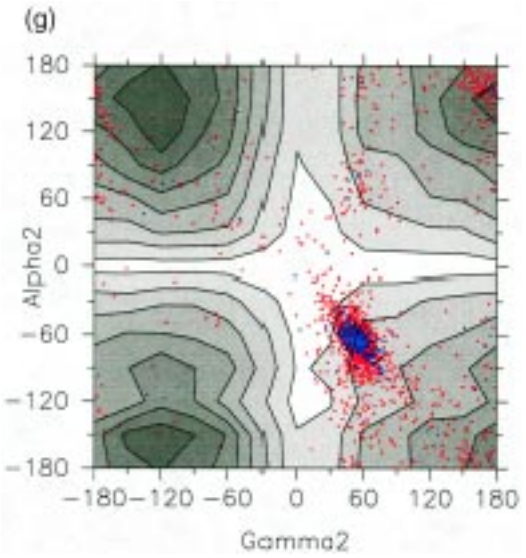

Figure 5. Significant conformational constraints on the α and ζ torsion angles that are absent in mononucleotides but are present in polynucleotides are elucidated in two-dimensional projections for the truncated dinucleotide. Electronic repulsion between the lone pair electrons on the phosphate ester oxygen atoms (O3′ and O5′), an additional local repulsive interaction not considered here, imposes additional restrictions on the conformation of the α^2 and ζ^1 torsion angles (Sudaralingam, 1969). As for mononucleotides, parameters describing the conformations about neighboring bonds (i.e. ε^1-ζ^1, ζ^1-α^2 and α^2-β^2) are interdependent while more distant parameters are not. Conformational data from the NDB is overlaid as in Figure 3. Although predicted preferred regions and *A*-form are not coincident, most of the moderate resolution (red) structures and nearly all of the highest resolution (blue) structures lie in allowed regions.

addressed now that a complete conformational map is available. There is a widely held belief that RNA molecules have substantial conformational flexibility because there are many single bonds in the backbone. Although wireframe models for nucleotides (Figure 1(a) and (b)) tend to reinforce this notion, examination of a CPK (Koltun, 1965) model (Figure 6) dispels this misleading impression and shows that only a small fraction of conformational space is free of severe steric overlaps. Specifically, using criteria chosen to be maximally inclusive, CDP and GDP are constrained to populate only 1.0 % and 3.9 % of the 7.5×10^9 potentially available conformations on a 20° grid, and the truncated dinucleotide is constrained to at most 4.9 % of its 1.2×10^{10} available grid conformations. It is anticipated that interactions between consecutive nucleobases will impose additional limitations on the conformational flexibility of polynucleotides. Furthermore, projections of these conformational spaces (Figures 3 and 5) show that most of these grid conformations can be grouped into a much smaller number of classes.

Two parameter projections (Figures 3 and 5) reveal that several pairs of parameters are interdependent (Figure 4). Generally, parameters which describe conformations about consecutive bonds (e.g. β and γ) are interdependent, while those that describe rotation about more distant bonds (e.g. β and ε) are not. Additionally, parameters describing rotation about bonds immediately proximal to the ribose ring (i.e.γ, ε and χ) depend on the ribose pucker and, to a lesser extent, on each other. These data suggest that many of the previously observed correlations between conformational parameters in

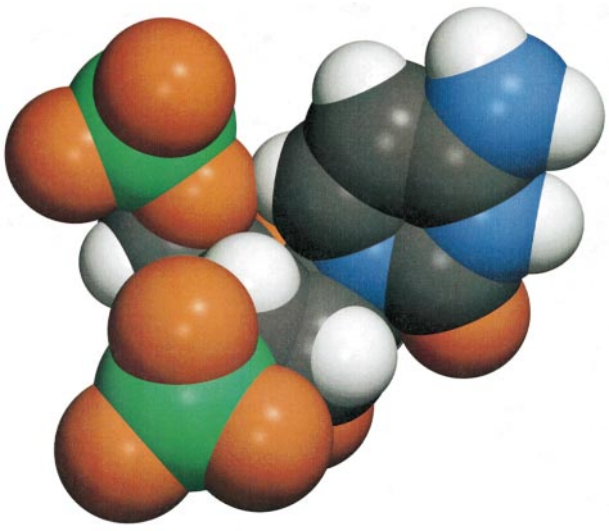

Figure 6. This CPK (Koltun, 1965) model of cytidine-5′,3′-diphosphate illustrates that despite the many single bonds present in RNA molecules, there are numerous steric barriers to rotation about these bonds. In particular, the conformations of the 5′ and 3′ phosphate groups and of the nucleobase are significantly constrained by the crowded ribose ring. Oxygen atoms are in red, carbon in grey, nitrogen in blue, hydrogen in white, and phosphorous in green. This Figure was prepared using POVChem (P. Thiessen, personal communication).

nucleic acids (Holbrook *et al*., 1978; Kitamura *et al*., 1981; Pearlman & Kim, 1986a; Kuszewski *et al*., 1997; Beckers & Buydens, 1998; Duarte & Pyle, 1998) are only present in stacked, repetitive structures and are probably not relevant to irregular structures such as loops.

Most remarkable, however, is the fact that a preference for *A*-form-like conformations is conspicuous in an analysis that uses only simple hard sphere steric exclusion. Discrete, well-defined conformational regions dominate all of the two-dimensional projections, suggesting that RNA conformations have a ''digital'' nature. Statistically preferred regions often include or abut large clusters of points that correspond to *A*-form conformers in X-ray crystal structures. This result implies that there is an entropic preference for *A*-form even in the isoenergetic limit where all attractive interactions are ignored. The widespread belief that *A*-form RNA structure is determined primarily by base-pairing, base-stacking and electrostatic interactions deserves re-evaluation, given that these factors seem to merely discriminate among the limited set of sterically available choices.

Acknowledgements

We thank Paul Thiessen, Rohit Pappu and Alan Grossfield for their critical reading of this manuscript and Paul Thiessen for assistance in preparing Figure 6. Supported by Hopkins' Medical Scientist Training Program GM07309 (V.L.M.) and by GM29548 (G.D.R.).

References

Altona, C. & Sundaralingam, M. (1972). Conformational analysis of the sugar ring in nucleosides and nucleotides. A new description using the concept of pseudorotation. *J. Am. Chem. Soc.* **94**, 8205-8212.

Berman, H. M., Olson, W. K., Beveridge, D. L., Westbrook, J., Gelbin, A., Demeny, T., Hsieh, S.-H., Srinivasan, A. R. & Schneider, B. (1992). The Nucleic Acid Database: A comprehensive relational database of three-dimensional structures of nucleic acids. *Biophys. J.* **63**, 751-759.

Brooks, B. R., Bruccoleri, R. E., Olafson, B. D., States, D. J., Swaminathan, S. & Karplus, M. (1983). CHARMM: a program macromolecular energy, minimization, and dynamics calculations. *J. Comput. Chem.* **4**, 187-217.

Beckers, M. L. M. & Buydens, L. M. C. (1998). Multivariate analysis of a data matrix containing A-DNA and B-DNA dinucleoside monophosphate steps: multidimensional Ramachandran plots for nucleic acids. *J. Comp. Chem.* **19**, 695-715.

Creamer, T. P. & Rose, G. D. (1994). α-Helix-forming propensities in peptides and proteins. *Proteins: Struct. Funct. Genet.* **19**, 85-97.

de Leeuw, H. P. M., Haasnoot, C. A. G. & Altona, C. (1980). Empirical correlations between conformational parameters in β-D-furanoside fragments derived from a statistical survey of crystal structures of nucleic acid constituents: full description of nucleoside molecular geometries in terms of four parameters. *Isr. J. Chem.* **20**, 108-126.

Duarte, C. M. & Pyle, A. M. (1998). Stepping through an RNA structure: a novel approach to conformational analysis. *J. Mol. Biol.* **284**, 1465-1478.

Gabb, H. A. & Harvey, S. C. (1993). Conformational transitions in potential and free energy space for furanoses and 2′-deoxynucleosides. *J. Am. Chem. Soc.* **115**, 4218-4227.

Giraldo, J., Wodak, S. J. & van Belle, D. (1998). Conformational analysis of GpA and GpAp in aqueous solution by molecular dynamics and statistical methods. *J. Mol. Biol.* **283**, 863-882.

Govil, G. (1976). Conformational structure of polynucleotides around the O-P bonds: refined parameters for CPF calculations. *Biopolymers,* **15**, 2303-2307.

Govil, G. & Saran, A. (1971a). Quantum chemical studies on the conformational structures of nucleic acids I: extended Hückel calculations on D-ribose phosphate. *J. Theor. Biol.* **30**, 621-630.

Govil, G. & Saran, A. (1971b). Quantum chemical studies on the conformational structures of nucleic acids II: EHT and CNDO calculations on the puckering of D-ribose. *J. Theor. Biol.* **33**, 339-406.

Guschlbauer, W. & Jankowski, K. (1980). Nucleoside conformation is determined by the electronegativity of the sugar substituent. *Nucl. Acids. Res.* **8**, 1421-1433.

Holbrook, S. R., Sussman, J. L., Warrant, R. W. & Kim, S.-H. (1978). Crystal structure of yeast phenylalanine transfer RNA II. Structural features and functional implications. *J. Mol. Biol.* **123**, 631-660.

Hopfinger, A. J. (1973). *Conformational Properties of Macromolecules*, Academic Press, New York.

Kim, S.-H., Berman, H. M., Seeman, N. C. & Newton, M. D. (1973). Seven basic conformations of nucleic acid structural units. *Acta Crystallog. sect. B,* **29**, 703-710.

Kitamura, K., Wakahara, A., Mizuno, H., Baba, Y. & Tomita, K. (1981). Conformationally ''concerted'' changes in nucleotide structures. A new description using circular correlation and regression analyses. *J. Am. Chem. Soc.* **103**, 3899-3904.

Koltun, W. L. (1965). Precision space-filling atomic models. *Biopolymers,* **3**, 665-679.

Kuszewski, J., Gronenborn, A. M. & Clore, G. M. (1997). Improvements and extensions in the conformational database potential for the refinement of NMR and X-ray structures of proteins and nucleic acids. *J. Mag. Res.* **125**, 171-177.

Lakshminarayanan, A. V. & Sasisekharan, V. (1969). Stereochemistry of nucleic acids and polynucleotides. V. Conformational energy of a ribose-phosphate unit. *Biopolymers,* **8**, 489-503.

Levitt, M. & Warshel, A. (1978). Extreme conformational flexibility of the furanose ring in DNA and RNA. *J. Am. Chem. Soc.* **100**, 2607-2613.

Newton, M. D. (1973). A model conformational study of nucleic acid phosphate ester bonds. The torsional potential of dimethyl phosphate monoanion. *J. Am. Chem. Soc.* **95**, 256-258.

Parkinson, G., Vojtechovsky, J., Clowney, L., Brünger, A. T. & Berman, H. M. (1996). New parameters for the refinement of nucleic acid containing structures. *Acta Crystallog. sect. D,* **52**, 57-64.

Pattabiraman, N. & Langridge, R. (1985). Flexibility of 3′,5′ deoxyribonucleoside diphosphates. *J. Biomol. Struct. Dynam.* **4**, 683-692.

Pearlman, D. A. & Kim, S.-H. (1985). Conformational studies of nucleic acids. II. The conformational energetics of commonly occurring nucleosides. *J. Biomol. Struct. Dynam.* **3**, 99-125.

Pearlman, D. A. & Kim, S.-H. (1986a). Conformational studies of nucleic acids. III. Empirical multiple correlation functions for nucleic acid torsion angles. *J. Biomol. Struct. Dynam.* **4**, 49-67.

Pearlman, D. A. & Kim, S.-H. (1986b). Conformational studies of nucleic acids. IV. The conformational energetics of oligonucleotides: d(ApApApA) and ApApApA. *J. Biomol. Struct. Dynam.* **4**, 69-98.

Pearlman, D. A. & Kim, S.-H. (1988). Conformational studies of nucleic acids. V. Sequence specificities in the conformational energetics of oligonucleotides: the homo-tetramers. *Biopolymers,* **27**, 59-77.

Perahia, D., Pullman, B. & Saran, A. (1974a). Molecular orbital calculations on the conformation of nucleic acids and their constituents IX: the geometry of the phosphate group: key to the conformation of polynucleotides?. *Biochim. Biophys. Acta,* **340**, 299-313.

Perahia, D., Pullman, B. & Saran, A. (1974b). Molecular orbital calculations on the conformation of nucleic acids and their constituents XI: the backbone structure of (3′-5′) and (2′-5′)-linked diribose monophosphates with different sugar puckers. *Biochim. Biophys. Acta,* **353**, 16-27.

Poltev, V. I., Milova, L. A., Zhorov, B. S. & Govyrin, V. A. (1981). Simulation of conformational possibilities of DNA *via* calculation of non-bonded interactions of complementary dinucleoside phosphate complexes. *Biopolymers,* **20**, 1-15.

Ponnuswamy, P. K. & Thiyagarajan, P. (1981). Conformational characteristics of the dimeric subunits of DNA from energy minimization studies. *Biophys. J.* **35**, 731-752.

Ramachandran, G. N. & Sasisekharan, V. (1963). Conformation of polypeptides and proteins. *J. Mol. Biol.* **7**, 95-99.

Saenger, W. (1984). *Principles of Nucleic Acid Structure*, Springer-Verlag, New York.

Saran, A. & Govil, G. (1971). Quantum chemical studies on the conformational structures of nucleic acids III: calculation of backbone structure by extended Hückel theory. *J. Theor. Biol.* **33**, 407-418.

Saran, A., Pullman, B. & Perahia, D. (1973a). Molecular orbital calculations on the conformation of nucleic acids and their constituents VI: conformation about the exocyclic C(4′)-C(5′) bond in α-nucleosides. *Biochim. Biophys. Acta.* **299**, 497-499.

Saran, A., Perahia, D. & Pullman, B. (1973b). Molecular orbital calculations on the conformation of nucleic acids and their constituents VII: conformation of the sugar ring in β-nucleosides: the pseudorotational representation. *Theor. Chim. Acta,* **30**, 31-44.

Sasisekharan, V. & Lakshminarayanan, A. V. (1969). Stereochemistry of nucleic acids and polynucleotides. VI. Minimum energy conformations of dimethyl phosphate. *Biopolymers,* **8**, 505-514.

Srinivasan, A. R., Yathindra, N., Rao, V. S. R. & Prakash, S. (1980). Preferred phosphodiester conformations in nucleic acids. A virtual bond torsion potential to estimate lone-pair interactions in a phosphodiester. *Biopolymers,* **19**, 165-171.

Sundaralingam, M. (1969). Stereochemistry of nucleic acids and their constituents IV: allowed and preferred conformations of nucleosides, nucleoside mono-, di-, tri-, tetraphosphates, nucleic acids and polynucleotides. *Biopolymers,* **7**, 821-860.

Tewari, R., Nanda, R. K. & Covil, G. (1974). Quantum chemical studies on the information structure of nucleic acids. IV. Calculation of backbone structure by CNDO method. *J. Theoret. Biol.* **46**, 229-239.

Thiyagarajan, P. & Ponnuswamy, P. K. (1981). Conformational charcteristics of dimeric subunits of RNA from energy minimization studies. *Biophys. J.* **35**, 753-769.

Tosi, C. & Lipari, G. (1981). Molecular orbital computations of the conformational energy of ethyl methyl phsophate. *Theor. Chim. Acta (Berlin),* **60**, 41-51.

Word, J. M., Lovell, S. C., LaBean, T. H., Taylor, H. C., Zalis, M. E., Presley, B. K., Richardson, J. S. & Richardson, D. C. (1979). Visualizing and quantifying molecular goodness-of-fit: small-probe contact dots with explicit hydrogen atoms. *J. Mol. Biol.* **285**, 1711-1733.

Yathindra, N. & Sundaralingam, M. (1973). Conformational studies on pyrimidine 5′-monophosphates and 3′,5′-diphosphates. Effect of the phosphate groups on the backbone conformation of polynucleotides. *Biopolymers,* **12**, 2261-2277.

Yathindra, N. & Sundaralingam, M. (1974). Backbone conformations in secondary and tertiary structural units of nucleic acids. Constraint in the phosphodiester conformation. *Proc. Natl Acad. Sci. USA,* **71**, 3325-3328.

Edited by I. Tinoco

(Received 27 April 1999; received in revised form 18 June 1999; accepted 18 June 1999)